

Short communication

# Anhydrous proton conductivity of a lamella-structured inorganic–organic zirconium–monododecyl phosphate crystalline hybrid

Je-Deok Kim <sup>a,\*</sup>, Toshiyuki Mori <sup>a</sup>, Itaru Honma <sup>b</sup>

<sup>a</sup> *Fuel Cell Materials Center, National Institute for Materials Science (NIMS),  
1-1 Namiki, Tsukuba, Ibaraki 305-0044, Japan*

<sup>b</sup> *National Institute of Advanced Industrial Science and Technology (AIST),  
Tsukuba, Ibaraki 305-8568, Japan*

Received 12 March 2007; received in revised form 14 May 2007; accepted 16 May 2007

Available online 21 May 2007

## Abstract

A lamella-structured inorganic–organic zirconium–monododecyl phosphate crystalline hybrid was investigated as an anhydrous proton conductor. Inorganic zirconium ions were coordinated by OH groups of a phosphate moiety from organic monododecyl phosphate. The inorganic–organic zirconium–monododecyl phosphate hybrid showed a lamella structure with crystalline ZrP, and the thermal stability increased up to 230 °C. A maximum proton conductivity of  $2 \times 10^{-3} \text{ S cm}^{-1}$  was obtained at 150 °C under anhydrous conditions. The high proton conductivity under high temperature and anhydrous conditions could be explained by considering the interaction between Zr ions and the phosphate group, and the phosphate concentration in the lamella-structured inorganic–organic zirconium–monododecyl phosphate hybrid.

© 2007 Elsevier B.V. All rights reserved.

**Keywords:** Inorganic–organic hybrid; Zirconium–monododecyl phosphate hybrid; Anhydrous proton conductor; High-temperature PEFC

## 1. Introduction

Polymer electrolyte fuel cell (PEFC) systems using hydrogen and oxygen gases have gained interest for use in stationary and non-stationary applications, because such systems are expected to provide higher energy efficiency and to be environmentally clean. Perfluorosulfonic polymers, such as Nafion<sup>®</sup>, have been developed over the past few years for use in PEFCs. The proton transport properties of these membranes strongly depend on the water content, and in practice, they are limited to operating temperatures below 90 °C for completely aqueous fuel cells. On the other hand, electrolytes that are tolerant to high temperatures (100–200 °C) have also been investigated as a result of the significant advantages afforded by the improved tolerance of Pt electrodes to carbon monoxide, the reduced resistance of electrodes and electrolytes, simplified heat management, and their ability to be co-generated [1]. Anhydrous proton-conducting electrolytes

can overcome these limitations. Several anhydrous electrolytes have been reported in the literature, among which are imidazole (pyrazole)–H<sub>2</sub>SO<sub>4</sub> [2], benzimidazole (Bz)–monododecyl phosphate (MDP) [3], 2-undecylimidazole–MDP [4], 1H-1,2,3-Triazole–H<sub>2</sub>SO<sub>4</sub> [5], Bz (1H-1,2,4-Triazole)–Nafion [6], polybenzimidazole (PBI)–H<sub>3</sub>PO<sub>4</sub> (H<sub>2</sub>SO<sub>4</sub>) [1,7,8], imidazole or Bz immobilization system [9], PAMA<sup>+</sup>H<sub>2</sub>PO<sub>4</sub><sup>−</sup> [10], and 3-glycidoxypolytrimethoxysilane–orthophosphoric acid [11]. The PBI–H<sub>3</sub>PO<sub>4</sub> electrolyte has been reported to exhibit good mechanical properties, to have low gas permeability and to be thermally stable above 100 °C [1]. However, this material is not easy to prepare and is not very soluble.

Here, we report the anhydrous proton conductivity of crystalline inorganic–organic zirconium–monododecyl phosphate (MDP) hybrids with a layered structure. Alberti and Casciola [12] have studied zirconium phosphonates as humidified proton conductors with layered  $\alpha$ - or  $\gamma$ -type structures. However, they report very poor conductivity ( $>10^{-6} \text{ S cm}^{-1}$ , at 200 °C) under anhydrous conditions. On the other hand, crystalline Zr-MDP inorganic–organic nano-hybrids did not have  $\alpha$ - and  $\gamma$ -type structures. The hybrids showed well-aligned layered structures, and a high proton conductivity

\* Corresponding author. Tel.: +81 29 860 4764; fax: +81 29 860 4667.  
E-mail address: [kim.jedeok@nims.go.jp](mailto:kim.jedeok@nims.go.jp) (J.-D. Kim).

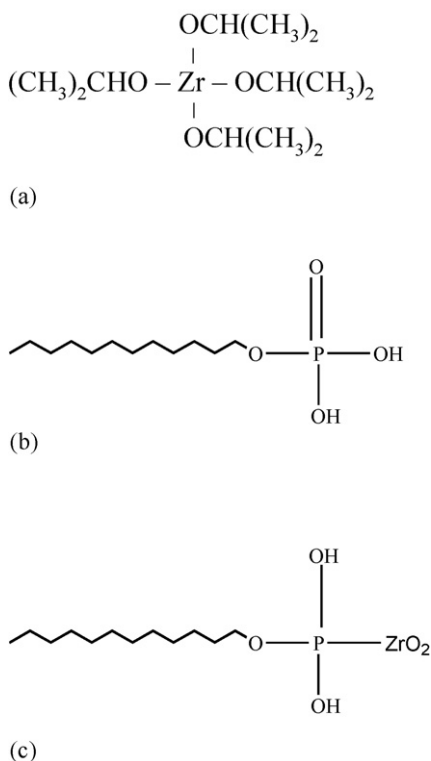


Fig. 1. Chemical structures of (a) zirconium isopropoxide, (b) monododecyl phosphate (MDP)  $\text{CH}_3(\text{CH}_2)_{11}\text{PO}_4\text{H}_2$ , and (c) Zr-MDP inorganic–organic hybrid structure.

of  $2 \times 10^{-3} \text{ S cm}^{-1}$  was obtained at  $150^\circ\text{C}$  under anhydrous conditions. We investigated the preparation and characterization of layered inorganic–organic zirconium–MDP hybrids using thermogravimetric-differential thermal analysis (TG-DTA), Fourier transform infrared spectroscopy (FTIR), X-ray diffraction (XRD), scanning transmission electron microscopy (STEM), and conductivity measurements.

## 2. Experimental

### 2.1. Materials

Zirconium isopropoxide solution ( $\text{Zr}(\text{OCH}(\text{CH}_3)_2)_4$ : 70 wt.% in 1-propanol) and MDP ( $\text{CH}_3(\text{CH}_2)_{11}\text{PO}_4\text{H}_2$  (Mw=266.31)) were purchased from Aldrich and Wako Chemical Co., Ltd., respectively. Fig. 1(a and b) show the chemical structures of zirconium isopropoxide and MDP, respectively. The end OH group of the phosphate in MDP can hybridize and/or interact with zirconium isopropoxide, resulting in the inorganic–organic zirconium–MDP hybrid structure (Fig. 1c). An ethyl acetoacetate solution was used with the zirconium isopropoxide to stabilize the sol and to prevent rapid hydrolysis. The inorganic–organic layered zirconium–MDP hybrids were synthesized in molar ratios (P/Zr) from 1:3 to 1:7. The solutions were cast in a Petri dish and subjected to thermal condensation at  $100^\circ\text{C}$  for 1 day to yield self-assembled hybrids. Element analysis of C–H–O and inductively coupled plasma–mass spectrometer (ICP–MS)

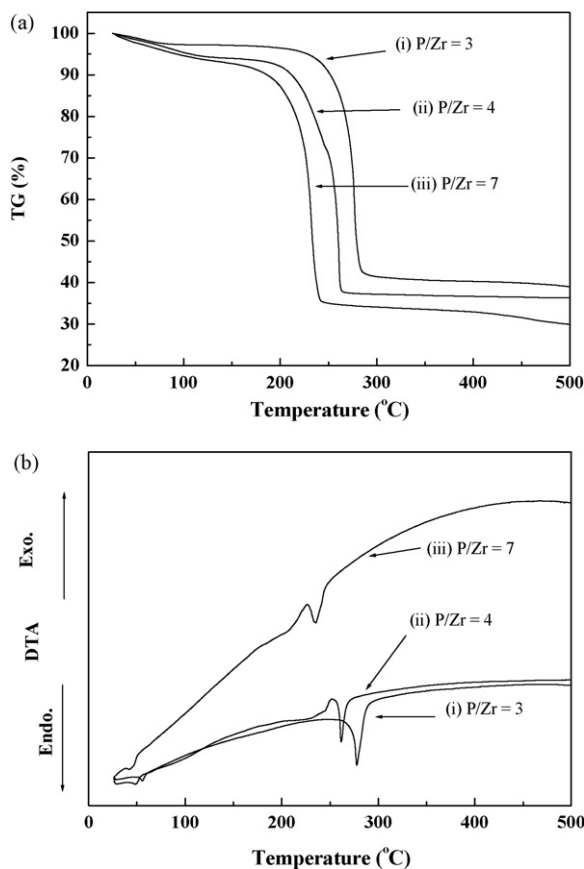


Fig. 2. (a) TG and (b) DTA analyses with different P/Zr molar ratios: (i) P/Zr = 3, (ii) P/Zr = 4, and (iii) P/Zr = 7.

showed that in the Zr–MDP hybrids, P/Zr = 2.73, 3.94, and 7.0 and that no ethyl acetoacetate reagent remained.

### 2.2. Characterization

The thermal stability of the hybrid materials was investigated by using TG-DTA (Model No. TG/DTA6200, SII Co. Ltd.). The samples were heated from room temperature to  $500^\circ\text{C}$  at a rate of  $5^\circ\text{C min}^{-1}$  under a  $\text{N}_2$  atmosphere.  $\text{Al}_2\text{O}_3$  powder was used as a reference material.

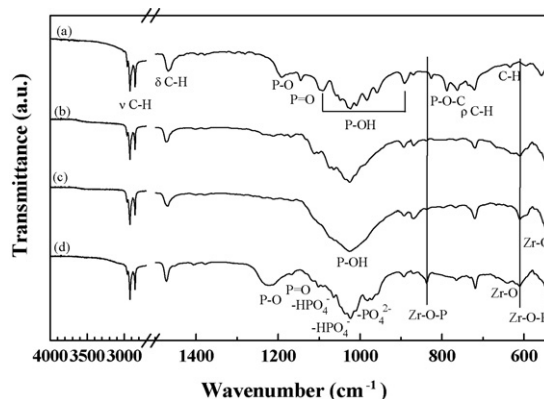


Fig. 3. IR spectra of the Zr–MDP hybrids: (a) pure MDP, (b) P/Zr = 3, (c) P/Zr = 4, and (d) P/Zr = 7.

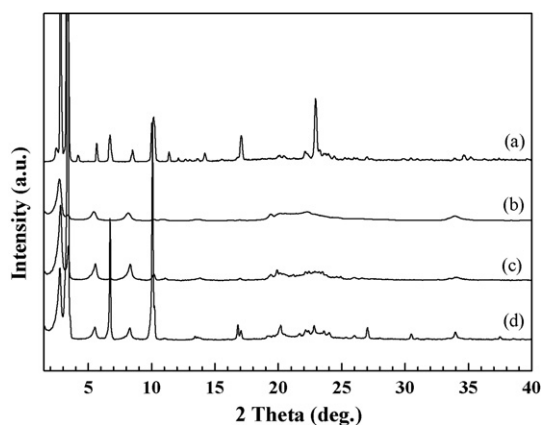


Fig. 4. XRD patterns of the Zr–MDP hybrids: (a) pure MDP (unknown) crystal, (b) P/Zr=3, (c) P/Zr=4, and (d) P/Zr=7.

Vibrational properties of the molecular structure were characterized by an attenuated total reflection (ATR) method using an infrared (IR) spectrophotometer (FT/IR-6200 with ATR PRO 410-S, JASCO).

XRD was used to determine and identify the physical structure of the samples as well as to indicate the degree of crystallinity. X-ray data were recorded on a Rigaku RINT-Ultima III/PC X-ray diffractometer using Cu K $\alpha$  radiation (1.5418 Å).

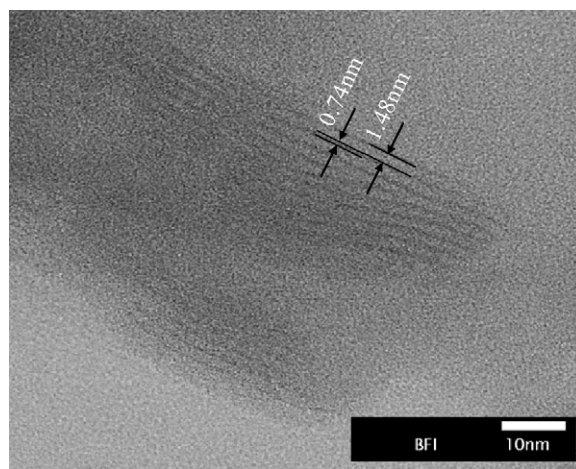
STEM images were taken of the specimens using a JEOL JEM-2100F operated at an accelerating voltage of 200 kV. Samples were crushed in an agate pestle and mortar and ultrasonically dispersed in ethanol prior to examination. The slurry was then coated onto a copper grid.

Proton conductivities were measured by using two-terminal impedance spectroscopy (SI 1260 Impedance Analyzer, Solatron). The hybrids were formed into pellets for the impedance measurements. Compact discs of the specimens were prepared by pressing at 6 tonnes cm $^{-2}$ . Disc samples with a diameter of 1 cm were placed between two ring-shaped gold plate blocking electrodes with an area of 0.2–0.4 cm $^2$ . The thickness of the pellets was between 0.2 and 1 mm depending on the powder volume. A frequency range of 1 Hz to 1 MHz and a peak-to-peak voltage of 100 mV were used for the impedance measurements. All of the cells were stabilized for 30 min at each temperature before performing the conductivity measurements. The proton conductivities were measured up to 150 °C under a flow of dry nitrogen (non-humidified).

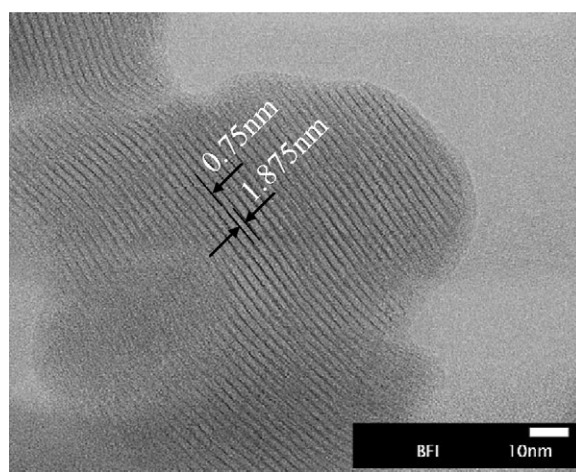
### 3. Results and discussion

Fig. 2(a and b) show TG-DTA analyses of Zr–MDP hybrid samples with P/Zr = 3, 4, and 7. The inorganic–organic hybrids with more Zr had a greater thermal stability. The endothermic peaks at 45, 49 and 56 °C in the DTA analyses were ascribed to the softness of MDP in the hybrids. In addition, the endothermic peaks at 235, 262 and 278 °C were ascribed to the evaporation of MDP in the hybrids. The hybrids were stable from 190 to 230 °C.

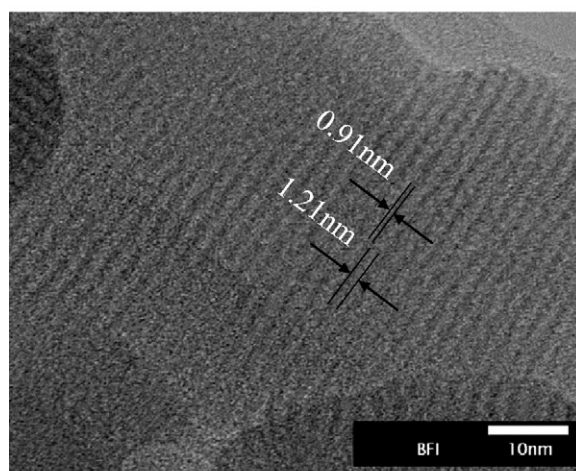
The vibration properties of the Zr–MDP inorganic–organic hybrid structure were characterized by using an ATR method on



(a)



(b)



(c)

Fig. 5. STEM images of the Zr–MDP hybrids: (a) P/Zr=3, (b) P/Zr=4, and (c) P/Zr=7.

an IR spectrophotometer. Fig. 3 shows the IR spectra for (a) pure MDP, and hybrids with (b) P/Zr = 3, (c) P/Zr = 4 and (d) P/Zr = 7. The C–H bending modes, which are typical of pure MDP, were assigned to the peaks at 2959–2853, 1466, 720 and 634 cm $^{-1}$ . The absorption bands due to the vibrations of the phosphate



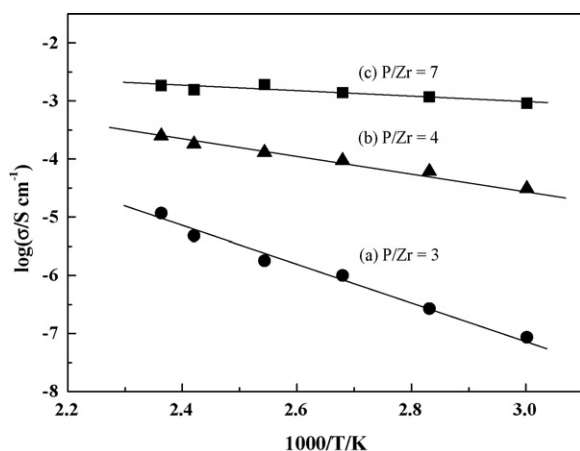


Fig. 6. Arrhenius plots ( $\log \sigma$  versus  $1000/T$ ) under anhydrous conditions of the inorganic–organic Zr–MDP hybrids with (a)  $P/Zr=3$ , (b)  $P/Zr=4$ , and (c)  $P/Zr=7$ .

group in the MDP molecule were observed at 1193 (P–O), 1140 (P=O), 1095–891 (P–OH), and 825–763  $\text{cm}^{-1}$  (P–O–C) [8]. On the other hand, the spectra of the inorganic–organic hybrids had new bands corresponding to Zr–O–P (836 and 610  $\text{cm}^{-1}$ ) and Zr–O (672, 640 and 547  $\text{cm}^{-1}$ ) [13]. Moreover, the peaks at 1193 and 1140 were absent in the spectra for the inorganic–organic hybrids with  $P/Zr=3$  and  $P/Zr=4$ , and in the spectrum for the hybrid with  $P/Zr=7$ , the P–O (1221  $\text{cm}^{-1}$ ) and P=O (1165  $\text{cm}^{-1}$ ) peaks were shifted. This means that there is a strong interaction between the phosphate groups (P=O and/or P–OH) and zirconium ions in the hybrids due to hydrolysis and thermal condensation. The  $P/Zr=4$  hybrid showed a single P–OH vibration at 1023  $\text{cm}^{-1}$ . Peaks for the  $-\text{HPO}_4^-$  and  $-\text{PO}_4^{2-}$  groups were observed at 1110, 1076 and 970  $\text{cm}^{-1}$  in the Zr–MDP hybrids [8,12].

Fig. 4 shows the XRD patterns of (a) pure MDP (unknown) crystal, and the hybrids with (b)  $P/Zr=3$ , (c)  $P/Zr=4$  and (d)  $P/Zr=7$ . The phases of the Zr–MDP hybrids were different from those of pure crystalline MDP and those of the  $\alpha$ -ZrP and  $\gamma$ -ZrP type structures [12]. The Zr–MDP hybrids showed both random lamellar and ZrP crystalline phases due to the interaction at the interface of the inorganic Zr ions and organic MDP. The intensity of crystalline reflection increased with an increase in the amount of MDP. Fig. 5 shows STEM images of the Zr–MDP hybrids. All samples showed a striped pattern, which is consistent with lamella structures.

Proton conductivities of lamella-structured Zr–MDP crystalline hybrids were determined by using ac impedance over the frequency range 1 Hz to 1 MHz under a flow of dry nitrogen. All of the cells were stabilized for 30 min at each temperature before performing the conductivity measurements. Fig. 6 shows Arrhenius plots ( $\log \sigma$  versus  $1000/T$ ) under anhydrous conditions of the inorganic–organic Zr–MDP hybrids with (a)  $P/Zr=3$ , (b)  $P/Zr=4$ , and (c)  $P/Zr=7$ . The conductivity of the Zr–MDP hybrids depended on both the temperature and  $P/Zr$  molar ratio and increased with an increase in  $P/Zr$ .

The activation energy of the hybrid with  $P/Zr=7$  ( $E_a=0.09$ ) was lower than that of the other hybrids ( $P/Zr=3$ ,  $E_a=0.63$ ;  $P/Zr=4$ ,  $E_a=0.26$ ). A maximum anhydrous proton conductivity of  $2 \times 10^{-3} \text{ S cm}^{-1}$  at 150 °C was obtained for the Zr–MDP hybrid with  $P/Zr=7$ , whereas pure crystalline MDP had a conductivity of  $3 \times 10^{-4} \text{ S cm}^{-1}$  at 120 °C due to the low thermal stability (m.p. = 110 °C) [3]. These proton conductivities generally obey the Arrhenius law, which indicates that the proton conduction is dominated by a thermal activation process. The proton conduction in the Zr–MDP hybrids is thought to be controlled by a hopping mechanism (proton jump). The proton conductivity of the hybrids might have originated due to the concentration of phosphate bonded at the interface of the Zr–MDP hybrids. Therefore, the high proton conductivity of the Zr–MDP hybrids at high temperature was due to ZrP interactions in the inorganic zirconium phase at the interface with organic MDP.

#### 4. Conclusions

Lamella-structured Zr–MDP crystalline hybrids were prepared by a sol-gel method involving self-assembly, and their proton conductivities were investigated under anhydrous conditions. The inorganic zirconium ions were coordinated by the phosphate groups in MDP. The crystalline Zr–MDP hybrids showed random lamella structures due to the MDP chains and also had a greater thermal stability due to the Zr inorganic phase. A high proton conductivity of  $2 \times 10^{-3} \text{ S cm}^{-1}$  at 150 °C under anhydrous conditions was obtained for the Zr–MDP inorganic–organic hybrids. In conclusion, incorporation of a proton conduction pathway at the interface of inorganic–organic hybrids is very important, and these hybrids are promising for use in PEFCs.

#### References

- [1] Q. Li, R. He, J.O. Jensen, N.J. Bjerrum, *Chem. Mater.* 15 (2003) 4896.
- [2] K.D. Kreuer, A. Fuchs, M. Ise, M. Spaeth, J. Maier, *Electrochim. Acta* 43 (1998) 1281.
- [3] J.D. Kim, I. Honma, *Solid State Ionics* 176 (2005) 979.
- [4] M. Yamada, I. Honma, *J. Phys. Chem. B* 108 (2004) 5522.
- [5] Z. Zhou, S. Li, Y. Zhang, M. Liu, W. Li, *J. Am. Chem. Soc.* 127 (2005) 10824.
- [6] J.D. Kim, T. Mori, S. Hayashi, I. Honma, *J. Electrochem. Soc.* 154 (2007) A290.
- [7] R. Bouchet, E. Siebert, *Solid State Ionics* 118 (1999) 287.
- [8] M. Kawahara, J. Morita, M. Rikukawa, K. Sanui, N. Ogata, *Electrochim. Acta* 45 (2000) 1395.
- [9] H.G. Herz, K.D. Kreuer, J. Maier, G. Scharfenberger, M.F.H. Schuster, W.H. Meyer, *Electrochim. Acta* 48 (2003) 2165.
- [10] A. Bozkurt, M. Ise, K.D. Kreuer, W.H. Meyer, G. Wegner, *Solid State Ionics* 125 (1999) 225.
- [11] K. Tadanaga, H. Yoshida, A. Matsuda, T. Minami, M. Tatsumisago, *Chem. Mater.* 15 (2003) 1910.
- [12] G. Alberti, M. Casciola, *Solid State Ionics* 97 (1997) 177.
- [13] J.D. Kim, T. Mori, I. Honma, *J. Electrochem. Soc.* 153 (2006) A508.